PCCP

Accepted Manuscript

This is an *Accepted Manuscript*, which has been through the Royal Society of Chemistry peer review process and has been accepted for publication.

Accepted Manuscripts are published online shortly after acceptance, before technical editing, formatting and proof reading. Using this free service, authors can make their results available to the community, in citable form, before we publish the edited article. We will replace this *Accepted Manuscript* with the edited and formatted *Advance Article* as soon as it is available.

You can find more information about *Accepted Manuscripts* in the **Information for Authors**.

Please note that technical editing may introduce minor changes to the text and/or graphics, which may alter content. The journal's standard **Terms & Conditions** and the **Ethical guidelines** still apply. In no event shall the Royal Society of Chemistry be held responsible for any errors or omissions in this *Accepted Manuscript* or any consequences arising from the use of any information it contains.

PCCP

PAPER

Unraveling the interplay between hydrogen bonding and rotational energy barrier to fine-tune the properties of triazine molecular glasses

Audrey Laventure,[a] Guillaume De Grandpré,[b] Armand Soldera,[b] Olivier Lebel*[c] and Christian Pellerin*[a]

Mexylaminotriazine derivatives form molecular glasses with outstanding glass-forming ability (GFA), high resistance to crystallization (glass kinetic stability, GS), and a glass transition temperature (T_g) above room temperature that can be conveniently modulated by selection of the headgroup and ancillary groups. A common feature of all these compounds is their secondary amino linkers, suggesting that they play a critical role in their GFA and GS for reasons that remain unclear because they can simultaneously form hydrogen (H) bonds and lead to a high interconversion energy barrier between different rotamers. To investigate independently and better control the influence of H bonding capability and rotational energy barrier on T_g, GFA and GS, a library of twelve analogous molecules was synthesized with different combinations of NH, NMe and O linkers. Differential scanning calorimetry (DSC) revealed that these compounds form, with a single exception, kinetically stable glasses with T_g values spanning a very broad range from -25 to 94 °C. While variable temperature infrared spectroscopy combined to chemometrics reveals that, on average, around 60% of the NH groups are still H-bonded as high as 40 °C above T_g, critical cooling rates obtained by DSC clearly show that molecules without H-bond donating linkers also present an outstanding GFA, meaning that H bonding plays a dominant role in controlling T_g but is not required to prevent crystallization. It is a high interconversion energy barrier, provoking a distribution of rotamers, that most efficiently promotes both GFA and resistance to crystallization. These new insights pave the way to more efficient glass engineering by extending the possible range of accessible T_g, allowing in particular the preparation of homologous glass-formers with high GS at ambient temperature in either the viscous or vitreous state.

Introduction

Organic glasses, by opposition to crystals, are amorphous materials that lack periodic order.[1] They possess various properties such as macroscopic homogeneity, transparency, better solubility and compositional flexibility, among others, that can be advantageously exploited in a wide array of (bio)materials applications. These organic amorphous materials can be prepared using either polymers or small molecules. The latter, also named molecular glasses, offer the advantages of being isomolecular and easier to purify than polymers, but they generally necessitate more extreme processing conditions to impede crystallization and they tend to crystallize faster over time, thus losing their advantageous properties. To cope with these issues, molecular glasses showing both an excellent glass-forming ability (GFA) and a high kinetic stability (glass stability, GS, *i.e.* resistance to crystallization) are therefore sought, particularly in the context of the rapid expansion of the organic electronics field and the need to optimize excipients in pharmaceutical products, two domains requiring materials that

readily form long-lived amorphous phases.[2,3] Unveiling the intimate link between molecular structure and these properties is thus of particular interest. Although the synthesis and characterization of libraries of compounds with natural poor packing and slow crystallization kinetics is one of the keys to unravel the challenging task of efficient glass design, limited work has been conducted on homologous series of organic compounds. In an attempt to relate the molecular properties and the bulk behavior of amorphous materials, different groups have studied the kinetics and the thermodynamics of glass formation in xylenes[4] and trisnaphtylbenzene isomers,[5] and more recently, in libraries of stilbenes[6] and trisarylbenzene analogues.[7]

While previous studies have usually focused on glass-forming molecules that can only interact by weak van der Waals interactions, Lebel and co-workers have introduced in 2006 a series of bis(mexyl)aminotriazine derivatives with outstanding GFA[8] that are capable of hydrogen bonding, a stronger intermolecular interaction that usually promotes crystallization and is widely used in crystal engineering to create predictably ordered and well-packed structures.[9,10] Over the last decade, more than 100 glass-forming triazine derivatives have been synthesized and characterized, successfully demonstrating that regularly-shaped and symmetrical compounds that can participate in hydrogen bonds can also readily form amorphous phases. Moreover, these aminotriazine compounds, shown in Scheme 1 (bearing two mexyl[§] ancillary groups), challenge the predictions of Wicker *et al.* based on a machine learning approach, which place them at the border of the crystalline and amorphous states.[11] These counterintuitive

a. *Département de chimie, Université de Montréal, Montréal, QC, H3C 3J7, Canada. E-mail : c.pellerin@umontreal.ca*
b. *Département de chimie, Université de Sherbrooke, Sherbrooke, QC, J1K 2R1, Canada.*
c. *Department of Chemistry and Chemical Engineering, Royal Military College of Canada, Kingston, ON, K7K 7B4, Canada. E-mail: olivier.lebel@rmc.ca*

features make aminotriazine derivatives an interesting model system to deepen our understanding of the glassy phase and of the molecular parameters leading to a good GFA. They also stand out as a model

Headgroup: X = NHMe or OMe
Linker: R, R' = NH, NMe or O
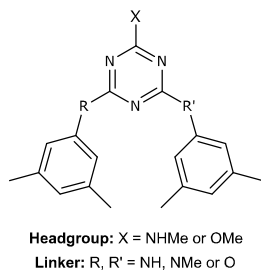
Scheme 1[‡]

system for experimental convenience: i) the vitreous phase of most of these compounds is kinetically stable for a relatively long time, limiting nucleation and growth of crystals during measurements (several of these compounds even resist crystallization in their supercooled liquid state for over 18 months upon annealing and even under shear stress);[12] ii) selection of the headgroup and ancillary groups enables tuning their glass transition temperature (T_g) values over a wide temperature range from 19 to 131 °C; and iii) their excellent GFA allows applying a slow cooling rate, thus enabling *in situ* characterization using techniques with relatively low temporal resolution.

The role of the headgroup and the ancillary groups of these molecules has been extensively studied previously.[13,14] In contrast, little is known about the influence of the groups linking the triazine core to the ancillary groups (R and R' linkers in Scheme 1) on the GFA, GS and T_g of these compounds. Indeed, secondary amines (NH) have been employed almost systematically as linkers until now; their H-bond donor character and/or their high rotational energy barrier may thus be critical in explaining the excellent GFA and high T_g for the numerous analogues synthesized so far. Indeed, studies of the headgroup structure have revealed that both hydrogen bonding and a high rotational barrier, along with steric bulk, promote glass formation and modulate T_g,[15,16] but it is yet unclear how the interplay between these three parameters influences glass formation and T_g for the ancillary group linkers. In the only attempt so far, substituting both NH groups by oxygen atoms has resulted in crystallization within less than 24 hours at ambient temperature.[8] This high propensity to crystallize was assumed to be a consequence of the absence of self-assembly by hydrogen bonding,[8] but it could also be due to a lower rotational barrier for the aryloxy groups, which are less strongly conjugated to the triazine ring than arylamino groups and can thus rearrange more easily to an ordered packing.[16] It is thus crucial to undertake a more systematic study of the impact of the ancillary linkers on GFA, GS and T_g to determine the contribution of each molecular parameter to these properties. Furthermore, being able to retain the excellent GFA and resistance to crystallization without using NH groups as linkers would give access to materials with a lower T_g range while retaining the demonstrated synthetic flexibility of these triazine derivatives, allowing their functionalization with different headgroups and ancillary groups, and thus opening the door to new exciting functional materials being in their viscous state at ambient temperature.

In this work, the impact of the linkers on glass formation is probed systematically by synthesizing and characterizing a new library of 12 compounds featuring three different linkers: NH, NMe and O. The elimination of the H-bond donor capability (*vs.* the reference compound with R = R' = NH) by replacing the NH linkers either by the isosteric but more freely rotating O group, or by the isoelectronic and sterically hindered NMe group revealed that H-bonding interactions at the linker location do not stand as a requirement for the spontaneous formation of long-lived glasses, but rather shows that a high rotational barrier is necessary to prevent crystallization. On the other hand, decreasing the number of hydrogen-bonding groups resulted in a sharp decrease of T_g, leading to kinetically stable glasses with T_g values as low as -25 °C. Combining variable-temperature infrared (IR) spectroscopy and chemometrics analyses revealed quantitative relationships between the T_g and the average number of bonded NH groups at T_g and the enthalpy of H-bond formation. Relations between T_g and GFA were also found for glass-formers with linkers that cannot lead to H-bond and are rationalized by taking into account both the rotational energy barrier around the linker and the nature of the intermolecular interactions involved. These structure-properties relationships provide valuable insight towards establishing unified guidelines for the engineering of stable functional glasses with tunable thermal properties.

Results and discussion

The compounds studied herein (Scheme 1) all share the same triazine core and bis(3,5-dimethylphenyl) ancillary groups. By exploiting all the combinations of available linkers (NH, NMe and O) and headgroups (NHMe or OMe), the library is composed of two series of six compounds for each headgroup. Scheme 2 highlights that this group of linkers enables a systematic investigation of the influence of hydrogen bonding, rotational energy barrier, and steric bulk separately. Indeed, both the O and NMe linkers cannot donate hydrogen bonds, as opposed to the NH linker. On the other hand, the NMe linkers are expected to present a high rotational energy barrier similar to that of the NH linkers, due to electron delocalization with the triazine ring, while it should be lower for the O linkers.
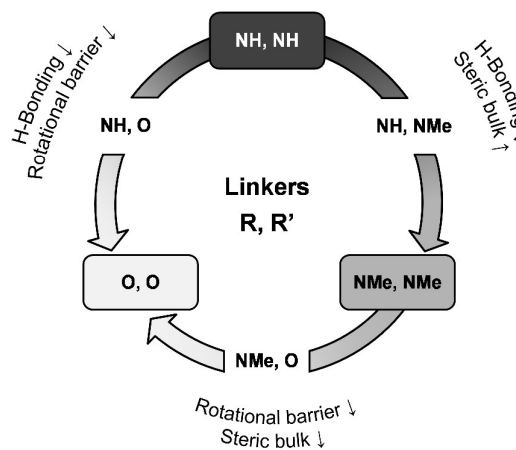
Scheme 2

Finally, the NH and O linkers are isosteric, while the NMe linker is bulkier. More specifically, in the sequence NH,NH → NH,O → O,O, shown on the left side of Scheme 2, the H-bonding possibility decreases while retaining a similar steric hindrance but lowering the rotational energy barrier. Changing the linkers from NH,NH to NH,NMe to NMe,NMe also provides a gradual decrease of the number of H-bond donors without affecting much the rotational barrier but this time combined with an increase in the steric hindrance. Finally, the sequence NMe,NMe → NMe,O → O,O completes the cycle, allowing the comparison of non H-bonded linkers with a larger or smaller steric hindrance and, as shown below, rotational energy barrier.

Synthesis

The reference compounds **1** and **2** with two NH linkers and a NHMe and a OMe headgroup, respectively, were synthesized according to literature procedures, as well as the cyanurate **3** with two O linkers and a OMe headgroup.[8]
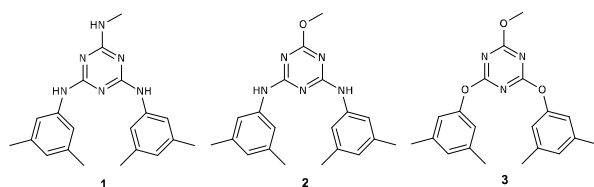
Mexyloxytriazine derivatives **4**-**6** were prepared in 47-74 % yield from the corresponding chlorotriazine derivatives and 3,5-dimethylphenol in the presence of K_2CO_3 in refluxing dioxane (Scheme 3), in a procedure similar to the one used to synthesize cyanurate **3**.[8] The products could be conveniently purified by dissolving in dichloromethane followed by washing with aqueous NaOH to remove the excess of 3,5-dimethylphenol and salts, any triazine impurities generated during the reaction being insoluble in dichloromethane. N-Methylmexylaminotriazine derivatives with a NHMe headgroup **7**-**8** were synthesized in 48-77 % yield from the corresponding chlorotriazines with a slight excess of N,3,5-trimethylaniline in refluxing dioxane (Scheme 4). Removal of the excess of N,3,5-trimethylaniline by aqueous acid washing followed by neutralization gave pure compounds **7**-**8**. However, for compounds with a OMe headgroup, this route proved unsuccessful as the methoxy group hydrolyzed during the reaction. Instead, methoxy-substituted N-methylated compounds **9-12** were synthesized from their NH analogues by methylation with sodium hydride and iodomethane in DMF (Scheme 5). Bis-mexylaminotriazine **2** could be converted to either mono-N-methyl derivative **9** or di-N-methyl analogue **10** depending on the conditions of the reaction. For compound **10**, conversion was near quantitative
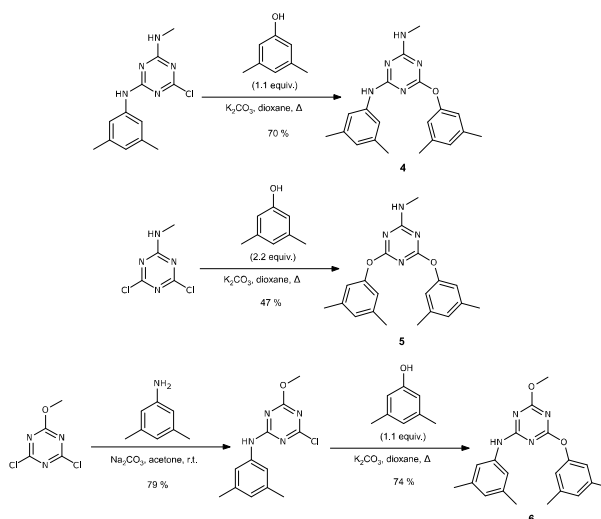
Scheme 3
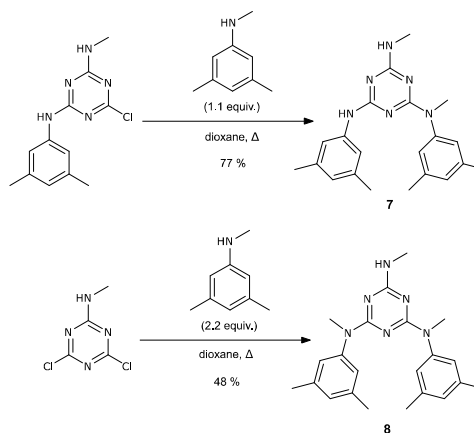
Scheme 4

and the compound could be conveniently purified by filtration on a short silica pad, while mono-N-methyl derivatives **9**, **11** and **12** could all be purified by recrystallization from hot hexanes. Interestingly, for compound **11**, the methylation was regioselective to the mexylamino group, and the NHMe headgroup did not impact the outcome of the reaction in a significant fashion.
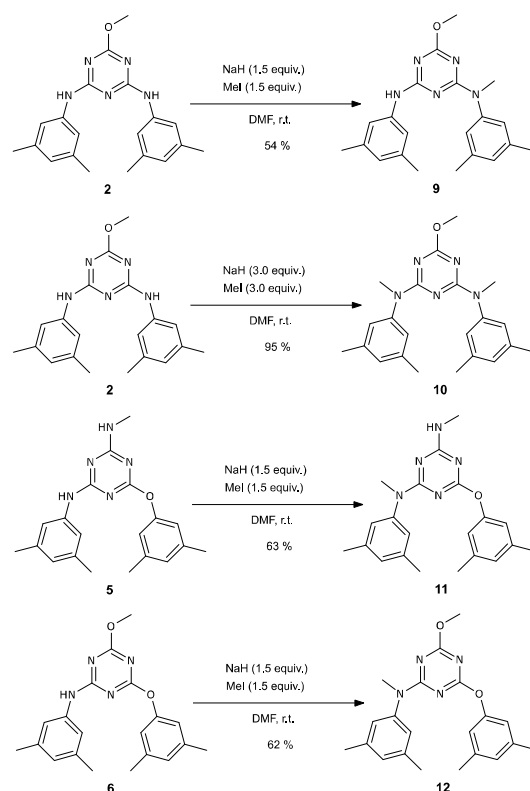
Scheme 5

Thermal properties

Differential scanning calorimetry (DSC) revealed that eleven out of the twelve compounds studied herein present an outstanding GFA, being completely amorphous (within DSC detection limit) after cooling from the melted state as slowly as 0.5 °C/min. The only exception is compound NHMe/O,O (**5**) (from this point, to simplify the referencing, compound identification numbers will be preceded by X/R,R', where X is the headgroup and R,R' are the linkers) whose critical cooling rate, *i.e.* the slowest rate at which a molecule can be cooled without presenting any traces of crystallization, is faster than 100 °C/min. This increase in critical cooling rate by at least a factor of 200 was not observed for compounds substituted with a OMe headgroup and for another library of compounds with phenyl ancillary groups instead of mexyl groups (see Supplementary Information, Scheme S1 for synthetic procedures and Fig. S1 for T_g), reinforcing the conclusion that the behavior of NHMe/O,O compound **5** is an isolated case. These results show for the first time that H-bonds are, in fact, not necessary to prepare molecular glasses with excellent GFA from triazine derivatives.

Fig. 1 shows that the linkers play an extremely important role on the thermal properties of the molecules, their T_g spanning from -25 to 94 °C (also see Table S1 in SI). Indeed, classifying the T_g values in ascending order clearly shows that the sequence of linker pairs follows the same order for the series with NHMe (in blue) and OMe (in orange) headgroups. Compounds featuring the NHMe headgroup always present a higher T_g than their OMe analogues. On average, this difference is 27 °C, which is close to the previously observed 29 °C average difference between analogues with NHMe and ethyl (Et) headgroups.[14] This difference in T_g is expected since

the NHMe group is a H-bond donor and is strongly conjugated to the triazine core, thus increasing the strength of intermolecular interactions and hindering its rotation compared to the OMe and Et groups. Interestingly, substituting a NH linker for an O or a NMe lowers T_g by the same magnitude, with an average of 31 °C, showing the large impact of the H-bond donating character of the linkers on T_g. The series of phenyl-substituted compounds (*vide supra*, Fig. S1 in SI) present T_g values very similar to those of their mexyl-substituted analogues, confirming the important role of the linkers on T_g. Two additional qualitative trends can be observed in Fig. 1. First, T_g increases with the number of NH groups (NMe,NMe < NH,NMe < NH,NH and O,O < NH,O < NH,NH) as previously reported by Naito[17] and van der Sman[18] for glassy H-bonded systems. Second, and more surprisingly, O linkers lead to higher T_g values than NMe linkers (NMe,NMe < NMe,O < O,O) despite their weaker conjugation to the triazine ring, possibly due to their smaller size (the sterically hindered NMe linkers
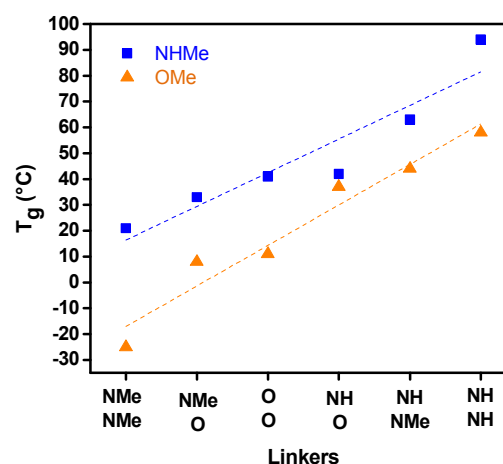
Fig. 1 T_g of the compounds with the NHMe (blue) or OMe (orange) headgroup and different linkers.

can obstruct hydrogen bonding with the triazine N atoms for compounds with the NHMe headgroup) or dipolar interactions.

Linker groups also influence the kinetic glass stability of the compounds. Indeed, cold crystallization was observed by DSC for compounds OMe/O,O (**3**), NHMe/O,O (**5**), NHMe/NH,O (**4**), NHMe/NMe,O (**11**) and OMe/NH,NMe (**9**) (see Table S1 in SI). In fact, the only compounds containing a O linker that did not show any crystallization by DSC are OMe/NH,O derivative **6** and its OMe/NMe,O analogue **12**, though both compounds crystallized over two weeks on standing at ambient temperature. In sharp contrast, OMe/NMe,NMe derivative **10**, which shows the lowest T_g value in the series, is kinetically stable at ambient temperature, which is close to 50 °C above its T_g, for more than a year. In comparison, its analogue OMe/NH,NH (**2**) crystallizes within three days upon annealing at 50 °C above its T_g. These features make the compounds with NMe linkers extremely competitive compared to other low T_g molecular glasses: in contrast to them, no long alkyl chain[19] or silyl ether[20] groups need to be introduced in their structure to impede crystallization. This represents a step forward in the study of homologous glass-formers, limiting the need to take into account the influence of supplementary structures introduced to extend the range of T_g.

IR spectroscopic characterization of H-bonded glasses

IR spectroscopy is a technique of choice to investigate hydrogen bonding *in situ* during cooling because of its chemical selectivity and its sensitivity to the environment and changes in interactions.[21] For instance, Tang *et al.* have correlated the NH stretching frequency to the hydrogen bonding strength and patterns in analogous amorphous pharmaceutical compounds.[22] Others working on organic OH-containing glass-former systems (sugars, 2-biphenylmethanol) have monitored *in situ* the frequency shift of the "bonded" and the "free" OH vibrations as a function of temperature and observed a break of slope at T_g, revealing that the rate of H-bond formation changes between the viscous and glassy states.[23,24] Series of temperature-controlled IR spectra were thus recorded upon cooling at 2 °C/min for the compounds with at least one NH group with the exception of NHMe/O,O (**5**) since its critical cooling rate is too fast (> 100 °C/min) to allow IR measurements with sufficient signal-to-noise ratio without inducing partial crystallization. Fig. 2 shows a representative example for NHMe/NH,NH compound **1** (T_g = 94 °C), displaying the mid-IR spectral region corresponding to the "free" and "bonded" NH (around 3407 and 3280 cm^{-1}, respectively) and the aromatic and aliphatic CH (3050-2850 cm^{-1}) stretching vibrations. It should be noted that the "free" and "bonded" labels are used for simplicity and should be understood as NH groups "strongly" and "weakly" H-bonded, respectively. Upon cooling from 130 to 40 °C, the principal changes occur in the NH stretching region as pinpointed by the arrows: the absorbance of the band corresponding to the "free" NH species decreases while that of the "bonded" NH species increases, meaning that a larger fraction of the NH groups are strongly H-bonded in the glassy state than in the viscous state.

In the past, we have observed changes in the relative amounts of "bonded" and "free" NH groups for triazine derivatives that resulted in a break in slope at T_g when plotting the absorbance ratio as a function of temperature. This conclusion was based on relative or semi-quantitative analysis, at best. Here, we aim to obtain for the first time quantitative information on the H-bonded species during
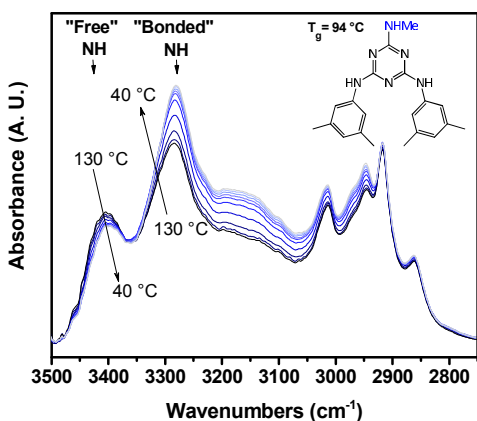
Fig. 2 Infrared spectra of the NHMe/NH,NH compound **1** (shown in the inset) recorded upon cooling highlighting the variation of the "free" and "bonded" NH bands with temperature.
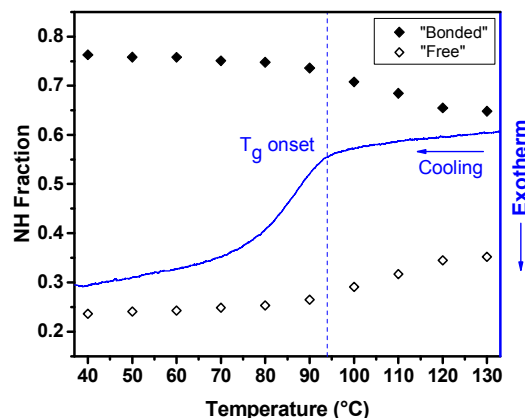
Fig. 3 Evolution of the "free" and the "bonded" NH fractions (black, left Y axis) with temperature during cooling at 2 °C/min for NHMe/NH,NH compound **1**. A DSC trace recorded at the same rate is superimposed (blue, right Y axis).

the vitrification of triazine derivatives and to relate it to their macroscopic properties, such as their T_g and enthalpy of H-bond formation. Chemometrics analysis is an appealing method in this context since traditional univariate analysis is not sufficient to obtain an absolute fraction of H-bonds because the "free" and the "bonded" NH stretching bands (besides the Fermi resonance band)[25] are broad and overlapped, making difficult their band fitting or direct integration. This statistical tool processes the data in a multivariate fashion to capture only the significant changes contained in the input variables, simplifying the extraction of the desired information.[26] A self-modeling multivariate curve resolution (MCR) approach was chosen, the Self-Modeling Mixture Analysis (SMMA), because it requires no prior knowledge of the species quantified (spectra for the pure "free" and "bonded" species are not necessary).[27,28] For instance, this approach was successfully used to study quantitatively the H-bond breaking dynamics of water upon heating.[29-31] A linear combination of pure "free" and "bonded" spectra, generated by the algorithm, is then used to reconstruct the experimental spectra and to evaluate the fraction of each species. Such analysis provides a good picture of the behavior of H-bonds upon thermal changes, even though it consists in a simplified model of the more realistic distribution of bond strengths within the material.[32]

The results of the calculations (details on the mathematical process can be found in the SI in Figs. S2 and S3) for NHMe/NH,NH derivative **1** are shown in Fig. 3, where the "bonded" and "free" NH fractions (left black Y axis) are plotted as a function of temperature (data were recorded during cooling). At temperatures above T_g, in the viscous state, approximately 65% of the NH groups are "bonded" and 35% are "free". Upon cooling below T_g, the percentage of "bonded" NH increases to reach 75%, leaving only 25% of "free" NH groups in the glassy state. In both curves, a change of slope can be observed around 95 °C, which corresponds to the T_g of the compound (94 °C), clearly showing that the glass transition occurs upon cooling when the fraction of H-bonded NH groups almost stops increasing. To reinforce this correspondence, a DSC scan recorded upon cooling at 2 °C/min (same rate as used to record the IR spectra) is superimposed on Fig. 3 to allow comparing the H-bonding and the bulk relaxation dynamics of the sample. An

ARTICLE

Journal Name

excellent agreement is observed between the spectroscopic T_g and the onset of the DSC T_g, suggesting that the compound becomes more and more viscous as the temperature is lowered and tends to jam while undergoing glass transition when a sufficient amount of H-bonds is formed. Once in the glassy state, the mobility is severely reduced, limiting the formation of additional H-bonds and explaining the quasi-plateau observed below T_g. The fact that 65% of the NH groups are still strongly H-bonded in the viscous state for NHMe/NH,NH compound **1** (the other compounds show similar fractions, between 55 and 75% at T_g + 40 °C, see Table S2 in SI), is well in line with our previous suggestion, based on qualitative results,[14,15,33] that the presence of H-bonds holding together the molecules above T_g thwarts crystallization upon cooling by preventing their reorganization into a crystalline lattice in the supercooled liquid.

Even though the type of H-bonded pattern (aggregates or network) found in H-bonded samples and the number of molecules involved in such structures are still sources of debate in the literature, interesting comparisons between the fractions obtained here and in other studies can be made. The large amount of "bonded" NH groups observed above T_g is not surprising considering that it has been estimated by IR spectroscopy that 26% of NH groups were still bonded in Nylon-6,6 above its melting point.[34] Moreover, in their IR study of alcohols, Barlow *et al.* have raised the idea that the fraction of H-bonded species must reach a value lying between 0.6 and 0.7 to allow the formation of aggregates (composed of chains or ring structures) in the liquid or supercritical state.[35] This threshold is close to the "bonded" NH fraction observed in our system at the T_g onset, when the system dynamics radically slows down. Moreover, the simulation work done by Harvey *et al.* on glassy imidazole oligomers,[36] probably the system closest to ours considering the possibility of NH⋯N interactions, led to fractions of H-bonded species both above and below T_g that correlate well with the values reported here, from 0.6 in the viscous state to 0.85 in the glassy phase (for equivalent temperatures relative to T_g)[37] indicating that SMMA provides reliable results and, most importantly, that the phenomena are more general than for the library we have studied.

To investigate if there is a quantitative relation between the fraction of "bonded" NH and the T_g of the compounds, we have multiplied the fraction of "bonded" NH calculated at the T_g of each compound by their respective number of NH groups. The results plotted in Fig. 4A show that T_g does indeed increase monotonically with the number of H-bonded NH groups per molecule for both the NHMe and OMe headgroup series, as highlighted by the blue and orange dotted lines, respectively. The compounds for which the number of H-bonded NH groups could not be measured by IR spectroscopy are also shown in Fig. 4A. For the compounds of the OMe series that do not bear NH linkers, it is clear that no H-bonds are present. For NHMe/O,O derivative **5** (crossed symbol), whose critical cooling rate was too fast for IR measurements, it is assumed that the average number of bonded NH groups is the same as for compound NHMe/NMe,NMe (**8**). In both cases, the data are in good agreement with the linear fits of T_g with the average number of "bonded" NH, supporting the validity of the calculations and the generality of the observed behavior. These observations are in good agreement with the work of van der Sman, where the T_g of carbohydrate derivatives was directly proportional to the number of available hydroxyl groups,[18] and also with the hypothesis made by Kaminski *et al.*[38] that H-bonds can increase the effective molecular weight of a compound, thus increasing its T_g.

Fig. 4 A) Evolution of T_g with the average number of "bonded" NH per molecule at T_g and B) evolution of T_g with the calculated absolute value of enthalpy ($|\Delta H|_{tot}$) of H-bond formation per molecule. The blue and orange dashed lines indicate the relationship between the variables for the NHMe and OMe headgroups, respectively. A crossed symbol is used for NHMe/O,O compound **5** since its average number of bonded NH groups and $|\Delta H|_{tot}$ of H-bond formation were assumed to be identical to those of NHMe/NMe,NMe compound **8**.

One should keep in mind that not only the number of intermolecular interactions influences the T_g; the strength of these interactions must also be taken into account to explain the differences in T_g values.[39] To investigate this relationship, the enthalpy of H-bond formation was calculated using the fractions of "free" and "bonded" NH found above T_g, where a thermodynamic equilibrium takes place as expressed by equation 1,[32] giving rise to the equilibrium constant of equation 2. Data below T_g cannot be used since the compounds do not reach equilibrium in the glassy state. Using the van't Hoff equation (3), the ΔH of H-bond formation can then be calculated. The linear fit for NHMe/NH,NH compound **1** is shown as a representative example in Fig. S4, where the slope leads to an absolute enthalpy value of 17 kJ/mol.

$$free\ NH \rightleftharpoons bonded\ NH \qquad (1)$$

$$K_{eq} = \frac{Bonded\ NH}{Free\ NH} \qquad (2)$$

$$lnK_{eq} = \frac{-\Delta H}{RT} + \frac{\Delta S}{R} \qquad (3)$$

Similar values are calculated for the other compounds (see Table S3 in SI) with an average of 15 kJ/mol. These enthalpies are in good agreement with the values reported for the formation of individual hydrogen bonds: NH···N and NH···O are classified at the border between "weak" and "strong" intermolecular interactions[9] with association energies of approximately 16 kJ/mol.[40] The total enthalpy per molecule ($|\Delta H|_{tot}$) can then be obtained by multiplying the average number of "bonded" NH at T_g by the $|\Delta H|$ of H-bond formation calculated for each compound. For NHMe/NH,NH compound **1**, the calculated $|\Delta H|_{tot}$ is 38 kJ/mol and is comparable to the value of 37 kJ/mol reported by Pawlus *et al.* for amorphous adonitol sugar bearing 3.5 effective OH groups.[41] The T_g of the compounds are plotted as a function of $|\Delta H|_{tot}$ in Fig. 4B. The value of T_g increases with enthalpy, confirming that it depends not only on the number of H-bonds but also on their strength. As in Fig. 4A, the non H-bonded compounds and the NHMe/O,O derivative **5** (crossed symbol) were added to the plot considering $|\Delta H|_{tot} = 0$ and the $|\Delta H|_{tot}$ of the NHMe/NMe,NMe compound **8**, respectively, to confirm the trend observed. However, it must be understood that while the triazine nitrogen atoms are the strongest electron donors

present and thus the most prevalent H-bond acceptors, a variety of NH···Y interactions are possible (Y = nitrogen or oxygen atom from another headgroup, from a linker, and from the triazine ring, without excluding possible weaker NH···π interactions with the mexyl or triazine rings) meaning that the calculated enthalpy of H-bond formation represents an average of all possibilities.[42-44]

Another striking observation in Fig. 4B is that for a similar enthalpy of H-bond formation per molecule, T_g is systematically higher for compounds with the OMe than the NHMe headgroup. This suggests that, in absence of H-bonds, other interactions take over and can also enable a good GFA. The comparison of Figs. 4A and 4B emphasizes this hypothesis: the OMe/NH,NH compound **2** has a similar average number (1.4-1.7) of "bonded" NH at T_g as its NHMe/NH,NMe (**1**) and
NHMe/NH,O (**4**) analogues that also contain two NH groups, but its $|\Delta H|_{tot}$ of H-bond formation is almost 25% lower. The same observation can be made by comparing the OMe and Et headgroup with two NH linkers. As mentioned in the Thermal properties section, while these compounds present, on average, the same T_g and have the same average number of bonded NH per molecule at T_g, *i.e.* 1.7 (the same chemometrics procedure was applied for the Et/NH,NH compound, not shown), the Et compound has a $|\Delta H|_{tot}$ that is 27% higher than the OMe one. This illustrates that a compound can present a higher T_g even if its $|\Delta H|_{tot}$ of H-bonds formation is lower, reinforcing the idea that H-bonds are not mandatory to achieve a glass-former design presenting a good GFA and a convenient T_g for devices used at or above room temperature.

Calculation of rotational energy barrier of non H-bonded linkers
The non H-bonded glass-formers with OMe headgroup and O and NMe linkers present, as expected, a lower T_g than their H-bonded

analogues, but they nevertheless possess a very good GFA. They can thus bring further fundamental insights on the impact on T_g and GFA of the rotation of the ancillary groups, which is closely related to the conformational flexibility that has been reported to be a parameter influencing the GFA.[45-47] *ab initio* calculations were conducted to estimate the activation energy required for rotating bonds between the linkers R or R' and the triazine core, as illustrated in the inset of Fig. 5. These simulations reveal that the O linkers have a much lower rotational energy barrier (20 kJ/mol) than the NMe linkers (54 kJ/mol). Fig. 5 shows a monotonic T_g decrease as the rotational energy barrier increases. As shown in previous studies, establishing a direct link between T_g and the rotational energy barrier is not straightforward and molecular dynamics simulations involving an assembly of molecules should be employed to specifically unveil the microscopic origin of variations of T_g, GFA, and GS.[16] Nevertheless, calculations on one molecule can lead to plausible interpretation. A
lower rotational energy barrier would allow the mexyl groups to adapt better to their environment above T_g, and thus to form more π-π interactions that lead to jamming at higher temperature, therefore leading to a higher T_g. A similar argument can be used for crystallization and can help explaining the much worse GFA of the NHMe/O,O compound **5** compared to all the other glasses. This compound needs a very rapid cooling rate, faster than 100 °C/min to prevent crystallization, while all its analogues yield a glass at cooling rates lower than 0.5 °C/min. In fact, both compounds with O,O linkers (with NHMe or OMe headgroup) present a poor resistance to crystallization, both on standing at ambient temperature and upon heating, and their crystallization temperature (Table S1) is 20 °C lower than for the other compounds of this library. These behaviors can be attributed to a faster sampling of different rotameric states by the mexyl groups allowing them to find the most thermodynamically stable one. In contrast, the much higher interconversion energy barrier of the NMe (or NH) linkers tends to favor the coexistence of multiple conformers, thereby preventing the molecules from organizing into an ordered crystalline structure.

These observations are consistent with the results for the compounds with a NHMe headgroup bearing non-H bonded linkers: they also show a higher Tg with O linkers than with NMe linkers for this series. In this case, the lower rotational barrier that is believed to lead to an easier formation of π-π interactions may also be combined to the better accessibility (lower steric hindrance) of the O linkers to accept an H-bond from the NH of the headgroup, or even to dipolar interactions between O linkers due to their additional lone pair of electrons compared to NMe linkers. For instance, it has been shown that strong intramolecular and weaker intermolecular O···O
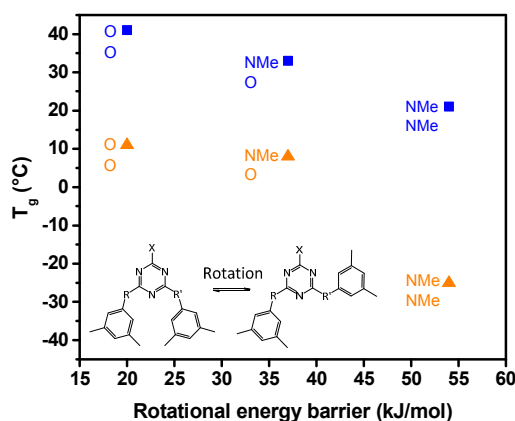
Fig. 5 Relation between the T_g and the calculated rotational energy barrier for the non H-bonded linkers. The inset shows the rotation of the ancillary group for which the energy barrier is simulated.

interactions are partly responsible for the planarity and face-to-face stacking in the single crystal structure of 2,6-dinitrophenol.[48] Such interactions could partly explain why compounds bearing O linkers show higher T_g than their NMe analogues even if their rotational barrier is lower.

Conclusions

This investigation of a homologous series of 12 glass-forming triazine derivatives bearing NH, NMe and O linkers provided new insights on the influence of H-bonding and interconversion energy barrier on the glass transition, glass-forming ability and glass kinetic stability. These compounds with excellent glass-forming ability (critical cooling rate lower than 0.5 °C/min for 11 compounds) present a T_g ranging from -25 to 94 °C, revealing the dramatic importance of delicate molecular modifications on glass properties. Variable-temperature infrared spectroscopy and chemometrics analysis were combined to monitor quantitatively for the first time H-bonding upon the vitrification of triazine derivatives. They revealed a monotonic increase of T_g with the average number of bonded NH groups at T_g and with the enthalpy of H-bond formation per molecule. The rotational energy barriers of the non H-bonded linkers were calculated and, as expected, indicated that the rotation of NMe linkers is significantly more hindered than that of O linkers. In spite of this, the T_g of compounds bearing O linkers was systematically higher than for those with NMe linkers, and their resistance to crystallization was lower. These observations lead to several conclusions that reinforce our understanding of the glass-forming behavior of this family of materials. In contrast to previous assertions, the presence of H-bonding groups contributes to glass formation (more than the half of the NH groups are still H-bonded even at 40 °C above their T_g) and to increasing T_g but is not necessary for glass formation. The existence and kinetic accessibility of multiple conformations of similar energies with hindered equilibria due to high rotational barriers is likely a more important contributor to glass-forming ability. For these reasons, headgroups or linkers that rotate more easily lead to a decrease in resistance to crystallization (worse kinetic stability). Finally, the presence of

hydrogen bonds, by raising T_g, hinders crystallization of the compound at ambient temperature, but actually promotes crystallization upon annealing above T_g. The lessons learned through the present study point towards NMe linkers as structural elements enabling to design glasses with low T_g values with long-term kinetic stability above their T_g. Such glasses show promise for applications involving materials in their viscous state, where few small molecules show a both an excellent glass-forming ability and high enough resistance to crystallization to be viable candidates.

Experimental section

General

2-Methylamino-4,6-dichloro-1,3,5-triazine,[8] 2-methoxy-4,6-dichloro-1,3,5-triazine,[49] 2-methylamino-4-mexylamino-6-chloro-1,3,5-triazine,[13] 2-methylamino-4,6-bis(mexylamino)-1,3,5-triazine (1),[8] 2-methoxy-4,6-bis(mexylamino)-1,3,5-triazine (2),[8] 2-methoxy-4,6-bis(3,5-dimethylphenoxy)-1,3,5-triazine (3),[8] 2-methoxy-4,6-bis(phenylamino)-1,3,5-triazine (13),[50] 2-chloro-4,6-bis(N-methylphenylamino)-1,3,5-triazine,[51] 2-(phenylamino)-4,6-dichloro-1,3,5-triazine,[52] and N,3,5-trimethylaniline[53] were prepared according to literature procedures. All other reagents and solvents were purchased from commercial sources and used without further purification. All reactions were performed under ambient atmosphere. SiliaFlash P60 grade silica gel and TLC plates were purchased from SiliCycle.

^{1}H NMR spectra were recorded on a Bruker Avance 400 MHz or a Varian Mercury 300 MHz at 298 K or 363 K (as indicated). ^{13}C NMR spectra were recorded on a Varian Mercury 300 MHz spectrometer at 298 K. FT-IR spectra were recorded on a Tensor 27 FT-IR spectrometer (Bruker Optics) equipped with a liquid nitrogen-cooled HgCdTe detector and a MIRacle (Pike Technologies) silicon attenuated total reflection (ATR) accessory as films directly cast on the ATR crystal from CH_2Cl_2 solution. Decomposition analyses of molecular glasses were obtained using a TGA 2950 thermogravimetric analyzer (TA Instruments) at a heating rate of 10 °C/min under a nitrogen atmosphere. The glass transition, crystallization and melting temperatures (T_g, T_c and T_m, respectively) were recorded by DSC with a PerkinElmer DSC 8500 calorimeter calibrated with indium using a heating rate of 10 °C/min. T_g values are reported as the average of the values observed in heating after an initial cycle of heating and cooling at 10 °C/min.

Variable-temperature infrared spectroscopy

Solutions of NH-substituted compounds in CH_2Cl_2 were spin-coated with a Headway Research EC-101 apparatus at 4000 rpm during 30 s on ZnSe windows. Variable-temperature transmission spectra were recorded, with a resolution of 4 cm^{-1}, using a Vertex 70 FT-IR spectrometer (Bruker Optics) equipped with a DTGS detector and a FTIR600 heating stage equipped with a T95 LinkPad temperature controller (Linkam Scientific Intruments). Samples were first heated to the highest temperature that did not induce dewetting or cold crystallization of the film, followed by a 3 min isotherm. Samples were then cooled down using a cooling rate of 2 °C/min and 100 scans were averaged for measuring each spectrum at each 10 °C. Background single beam spectra were recorded for each temperature. Principal component analysis and SMMA analysis were carried out using the PCA and the Purity algorithms, respectively, available in PLS_Toolbox (Eigenvector Research). Prior

to these analyses, spectra were preprocessed using the baseline correction and the normalization area options.

Calculation methodology

Calculations were carried out using the Density Functional Theory approach using B3LYP as the functional with the 6-31g(d,p) basis set in the Gaussian 09 © environment.[54] The *scan* keyword was used. To determine the potential energy barrier, a scan of the dihedral angle associated with the bond between the linker and the mexyl group, was undertaken. It consists in constraining this angle to a specific value. It is then incremented by steps of 10° between 0 and 180°. At each step, the geometry of the rest of the molecule is optimized in order to reach a minimum in energy. The rotational potential energy barrier corresponds to the energy that needs to be crossed to go from one state of minimum energy to the other (both minimum energy states are equal in energy).

Syntheses

2-Methylamino-4-mexylamino-6-(3,5-dimethylphenoxy)-1,3,5-triazine (4) 2-Methylamino-4-mexylamino-6-chloro-1,3,5-triazine (0.264 g, 1.00 mmol) was dissolved in dioxane (5 mL) in a round-bottomed flask equipped with a magnetic stirrer and a water-jacketed condenser. K_2CO_3 (0.152 g, 1.10 mmol) and 3,5-dimethylphenol (0.134 g, 1.10 mmol) were successively added, and the mixture was refluxed for 2 days. After allowing to cool down to ambient temperature, ethyl ether and H_2O were added, and the resulting precipitate was collected by filtration, washed with H_2O and ethyl ether, and allowed to completely dry to give 0.244 g of compound **4** in acceptable purity (0.698 mmol, 70 %). T_g 42 °C, T_c 122 °C, T_m 178 °C; FT-IR (ATR/CH_2Cl_2) 3384, 3274, 3149, 3014, 2950, 2919, 2859, 1617, 1579, 1554, 1530, 1464, 1393, 1348, 1244, 1192, 1189, 1172, 1090, 1038, 1000, 929, 888, 843, 811, 687, 662, 648 cm^{-1}; ^{1}H NMR (400 MHz, DMSO-d_6, 363 K) δ 8.98 (br s, 1H), 7.29 (s, 2H), 7.10 (br s, 1H), 6.86 (s, 1H), 6.80 (s, 2H), 6.60 (s, 1H), 2.88 (s, 3H), 2.30 (s, 6H), 2.19 (s, 6H) ppm; ^{13}C NMR (75 MHz, DMSO-d_6) δ 171.2, 170.8, 167.9, 167.7, 165.7, 165.1, 152.8, 140.1, 139.1, 137.6, 127.0, 124.0, 120.0, 117.9, 27.8. 27.6. 21.5. 21.2 ppm; HRMS (ESI, MNa$^+$) calcd. for $C_{20}H_{23}NaN_5O$ m/e: 372.1795, found: 372.1801.

2-Methylamino-4,6-bis(3,5-dimethylphenoxy)-1,3,5-triazine (5) 2-Methylamino-4,6-dichloro-1,3,5-triazine (1.00 g, 5.59 mmol) was dissolved in dioxane (20 mL) in a round-bottomed flask equipped with a magnetic stirrer and a water-jacketed condenser. K_2CO_3 (1.70 g, 12.3 mmol) and 3,5-dimethylphenol (1.50 g, 12.3 mmol) were successively added, and the mixture was refluxed for 2 days. After allowing to cool down to ambient temperature, the mixture was poured into H_2O and stirred 20 min at ambient temperature. The resulting precipitate was collected by filtration, washed with 1M aq. NaOH, H_2O and hexanes, and allowed to dry completely in air to give 0.924 g of pure compound **5** (2.64 mmol, 47 %). T_g 41 °C, T_c 58, 100 °C, T_m 180 °C; FT-IR (ATR/CH_2Cl_2) 3277, 3150, 3016, 2977, 2917, 2871,1640, 1619, 1598, 1580, 1553, 1468, 1437, 1416, 1385, 1368, 1288, 1254, 1175, 1146, 1083, 1036, 1000, 948, 925, 895, 850, 808, 739, 699, 680, 656, 643 cm^{-1}; ^{1}H NMR (300 Mhz, CDCl$_3$, 298 K) δ 6.83 (s, 2H), 6.79 (s, 2H), 6.74 (s, 2H), 6.27 (br s, 2H), 2.90 (d, ^3J = 4.1 Hz, 3H), 2.29 (s, 6H), 2.28 (s, 6H) ppm; ^{13}C NMR (75 MHz, CDCl$_3$) δ 172.5, 171.7, 168.8, 151.9, 151.8, 139.0, 138.8, 127.2, 127.1, 119.2, 27.8, 21.3 ppm; HRMS (ESI, MNa$^+$) calcd. for $C_{20}H_{22}NaN_4O_2$ m/e: 373.1635, found: 373.1644.

2-Methoxy-4-mexylamino-6-(3,5-dimethylphenoxy)-1,3,5-triazine (6) 2-Methoxy-4,6-dichloro-1,3,5-triazine (2.00 g, 11.1 mmol) was

dissolved in acetone (30 mL) in a round-bottomed flask equipped with a magnetic stirrer. Na_2CO_3 (1.18 g, 11.1 mmol) was added, then the flask was placed in an ice bath. A solution of 3,5-dimethylaniline (1.39 mL, 1.35 g, 11.1 mmol) in acetone (20 mL) was then slowly added at 0-5 °C under vigorous stirring, after which the ice bath was removed and the mixture was stirred for 1h at ambient temperature, after which H_2O was added. The product was extracted with ethyl ether, the organic layer was washed with brine, dried over Na_2SO_4, filtered, and the solvent was evaporated under reduced pressure. Recrystallization from hot hexanes afforded 2.31 g of the 2-methoxy-4-mexylamino-6-chloro-1,3,5-triazine precursor (8.73 mmol, 79 %). T_m 104 °C; FT-IR (ATR/CH_2Cl_2) 3360, 3279, 3235, 3190, 3142, 3008, 2951, 2917, 2866, 1618, 1557, 1487, 1457, 1389, 1364, 1281, 1205, 1171, 1095, 1046, 917, 881, 841, 808, 733, 682 cm^{-1}; ^{1}H NMR (300 MHz, CDCl$_3$, 298 K) δ 7.65 (br s, 1H), 7.17 (s, 2H), 6.80 (s, 1H), 4.02 (s, 3H), 2.32 (s, 6H) ppm; ^{13}C NMR (75 MHz, CDCl$_3$) δ 171.5, 170.6, 165.2, 138.7, 136.5, 126.7, 118.9, 55.5, 21.4 ppm; HRMS (ESI, MNa$^+$) calcd. for $C_{12}H_{13}ClNaN_4O$ m/e: 287.0670, found: 287.0681.

2-Methoxy-4-mexylamino-6-chloro-1,3,5-triazine (0.265 g, 1.00 mmol) was dissolved in dioxane (5 mL) in a round-bottomed flask equipped with a magnetic stirrer and a water-jacketed condenser. K_2CO_3 (0.152 g, 1.10 mmol) and 3,5-dimethylphenol (0.134 g, 1.10 mmol) were successively added, and the mixture was refluxed for 2 days. After allowing to cool down to ambient temperature, ethyl ether and H_2O were added, and both layers were separated. The organic layer was washed with 1M aqueous NaOH and brine, dried over Na_2SO_4, filtered, and the solvent was evaporated under reduced pressure and dried thoroughly to give 0.259 g of pure compound **6** (0.739 mmol, 74 %). T_g 37 °C; FT-IR (ATR/CH_2Cl_2) 3367, 3284, 3233, 3150, 3014, 2953, 2919, 2865, 1619, 1570, 1550, 1458, 1407, 1372, 1357, 1323, 1291, 1270, 1247, 1195, 1182, 1149, 1118, 1092, 1036, 1000, 973, 927, 889, 845, 814, 687, 660 cm^{-1}; ^{1}H NMR (400 MHz, DMSO-d_6, 363 K) δ 9.64 (br s, 1H), 7.20 (s, 2H), 6.92 (s, 1H), 6.84 (s, 2H), 6.66 (s, 1H), 3.94 (s, 3H), 2.31 (s, 6H), 2.17 (s, 6H) ppm; ^{13}C NMR (75 MHz, DMSO-d_6) δ 172.6, 172.4, 166.2, 152.4, 139.3, 139.0, 137.8, 127.6, 124.9, 119.8, 118.8, 117.9, 55.0, 21.2 ppm; HRMS (ESI, MNa$^+$) calcd. for $C_{20}H_{22}NaN_4O_2$ m/e: 373.1635, found: 373.1639.

2-Methylamino-4-mexylamino-6-(N,3,5-trimethylphenylamino)-1,3,5-triazine (7) 2-Methylamino-4-mexylamino-6-chloro-1,3,5-triazine (0.527 g, 2.00 mmol) was dissolved in dioxane (15 mL) in a round-bottomed flask equipped with a magnetic stirrer and a water-jacketed condenser. N,3,5-trimethylaniline (0.297 g, 2.20 mmol) were successively added, and the mixture was refluxed for 2 days. After allowing to cool down to ambient temperature, 1M aqueous HCl and CH_2Cl_2 were added, and both layers were separated. The organic layer was recovered, and hexanes was added until an off-white precipitate had completely formed. The precipitate was collected by filtration, washed with hexanes, and redissolved in CH_2Cl_2. The solution was washed with 1M aqueous NaOH, dried over Na_2SO_4, filtered, and the solvent was evaporated under reduced pressure and dried thoroughly to give 0.555 g of compound **7** (1.53 mmol, 77 %). T_g 63 °C; FT-IR (ATR/CH_2Cl_2) 3411, 3279, 3170, 3131, 3011, 2946, 2917, 2864, 1604, 1581, 1547, 1516, 1495, 1439, 1390, 1328, 1301, 1256, 1228, 1203, 1178, 1138, 1114, 1067, 1034, 999, 905, 891, 840, 809, 737, 710, 698, 690, 656 cm^{-1}; ^{1}H NMR (400 MHz, DMSO-d_6, 363 K) δ 8.33 (br s, 1H), 7.27 (s, 2H), 6.95 (s, 2H), 6.87 (s, 1H), 6.52 (s, 1H), 6.41 (br s, 1H), 3.43 (s, 3H), 2.85 (d, ^3J = 4.1 Hz, 3H), 2.30 (s, 6H), 2.15 (s, 6H) ppm; ^{13}C NMR (75

MHz, DMSO-d_6) δ 166.5, 165.8, 164.3, 145.5, 140.9, 138.2, 137.3, 127.5, 125.2, 123.0, 117.3, 38.1, 27.7, 27.4, 21.5, 21.3 ppm; HRMS (ESI, MNa$^+$) calcd. for $C_{21}H_{26}NaN_6$ m/e: 385.2117, found: 385.2124.

2-Methylamino-4,6-bis(N,3,5-trimethylphenylamino)-1,3,5-triazine (8) 2-Methylamino-4,6-dichloro-1,3,5-triazine (0.358 g, 2.00 mmol) was dissolved in dioxane (15 mL) in a round-bottomed flask equipped with a magnetic stirrer and a water-jacketed condenser. N,3,5-trimethylaniline (0.595 g, 4.40 mmol) were successively added, and the mixture was refluxed for 2 days. After allowing to cool down to ambient temperature, 1M aqueous HCl and CH_2Cl_2 were added, and both layers were separated. The organic layer was recovered, dried over Na_2SO_4, filtered, and the solvent was evaporated under reduced pressure and dried thoroughly to give 0.359 g of compound **8** (0.954 mmol, 48 %). T_g 21 °C; FT-IR (ATR/CH_2Cl_2) 3423, 3277, 3164, 3009, 2924, 2917, 2866, 1608, 1580, 1540, 1492, 1478, 1452, 1380, 1329, 1266, 1241, 1201, 1172, 1116, 1038, 919, 883, 845, 810, 702, 692, 664 cm^{-1}; ^{1}H NMR (300 MHz, CDCl$_3$, 298 K) δ 7.01 (s, 4H), 6.84 (s, 2H), 5.06 (br s, 1H), 3.46 (s, 6H), 2.82 (d, ^3J = 4.1 Hz, 3H), 2.33 (s, 12H) ppm; ^{13}C NMR (75 MHz, CDCl$_3$) δ 166.7, 165.6, 144.8, 137.7, 126.7, 124.2, 37.4, 27.4, 21.3 ppm; HRMS (ESI, MNa$^+$) calcd. for $C_{22}H_{28}NaN_6$ m/e: 399.2273, found: 399.2284.

2-Methoxy-4-mexylamino-6-(N,3,5-trimethylphenylamino)-1,3,5-triazine (9) 2-Methoxy-4,6-bis(mexylamino)-1,3,5-triazine (2.00 g, 5.72 mmol) was dissolved in anhydrous DMF (20 mL) in a flame-dried round-bottomed flask equipped with a magnetic stirrer. NaH (60 wt%, 0.206 g, 8.59 mmol) was added, and the mixture was stirred 30 min at ambient temperature until hydrogen evolution had stopped. Iodomethane (0.535 mL, 1.22 g, 8.59 mmol) was slowly added, and the mixture was stirred at ambient temperature for 12 h. The mixture was then poured into H_2O and stirred 20 min, then the precipitate was collected by filtration and abundantly washed with H_2O. The crude product was chromatographed on silica (AcOEt/Hexanes 1:4) to give 1.13 g of compound **9** (3.11 mmol, 54 %) as well as 0.241 g of bis(N,3,5-trimethylphenylamino) derivative **10** (0.638 mmol, 11 %). Alternatively, compound **9** could be isolated by recrystallization from hexanes, which gave 0.863 g (2.37 mmol, 42 %). T_g 44 °C; T_c 126 °C; T_m 148 °C; FT-IR (ATR/CH_2Cl_2) 3374, 3282, 3233, 3192, 3120, 3011, 2979, 2950, 2918, 2864, 1606, 1588, 1564, 1541, 1504, 1458, 1400, 1390, 1377, 1354, 1326, 1302, 1267, 1221, 1207, 1184, 1162, 1123, 1103, 1071, 1054, 1037, 999, 990, 932, 904, 888, 842, 812, 771, 715, 690, 655 cm^{-1}; ^{1}H NMR (400 MHz, DMSO-d_6, 363 K) δ 8.96 (br s, 1H), 7.24 (s, 2H), 6.96 (s, 2H), 6.92 (s, 1H), 6.57 (s, 1H), 3.87 (s, 3H), 3.45 (s, 3H), 2.30 (s, 6H), 2.15 (s, 6H) ppm; ^{13}C NMR (75 MHz, DMSO-d_6) δ 170.8, 166.9, 165.0, 144.6, 140.1, 138.4, 137.5, 128.2, 125.0, 123.9, 117.5, 54.0, 38.3, 38.2, 21.4, 21.3 ppm; HRMS (ESI, MNa$^+$) calcd. for $C_{21}H_{25}NaN_5O$ m/e: 386.1951, found: 386.1958.

2-Methoxy-4,6-bis(N,3,5-trimethylphenylamino)-1,3,5-triazine (10) 2-Methoxy-4,6-bis(mexylamino)-1,3,5-triazine (1.07 g, 3.06 mmol) was dissolved in anhydrous DMF (20 mL) in a flame-dried round-bottomed flask equipped with a magnetic stirrer. NaH (60 wt%, 0.367 g, 9.18 mmol) was added, and the mixture was stirred 30 min at ambient temperature until hydrogen evolution had stopped. Iodomethane (0.571 mL, 1.30 g, 9.18 mmol) was slowly added, and the mixture was stirred at ambient temperature for 12 h. Hexanes and H_2O were then added, and both layers were separated. The

aqueous layer was extracted twice with hexanes, the organic extracts were combined, washed with H_2O and brine, dried over Na_2SO_4, filtered, and the volatiles were evaporated under vacuum. Filtration on a short silica plug (AcOEt/Hexanes 1:4) gave 1.10 g of pure compound **10** (2.91 mmol, 95 %). T_g -25 °C; FT-IR (ATR/CH_2Cl_2) 3009, 2948, 2918, 2866, 1608, 1561, 1529, 1475, 1458, 1385, 1359, 1322, 1269, 1230, 1215, 1162, 1116, 1086, 1039, 1000, 983, 950, 915, 881, 847, 811, 749, 727, 702, 662 cm^{-1}; ^{1}H NMR (300 MHz, CDCl$_3$, 298 K) δ 6.95 (s, 4H), 6.85 (s, 2H), 3.81 (s, 3H), 3.45 (s, 6H), 2.31 (s, 12H) ppm; ^{13}C NMR (75 MHz, CDCl$_3$) δ 170.9, 166.5, 144.3, 137.9, 127.3, 124.2, 53.7, 37.8, 21.3 ppm; HRMS (ESI, MNa$^+$) calcd. for $C_{22}H_{27}NaN_5O$ m/e: 400.2108, found: 400.2117.

2-Methylamino-4-(N,3,5-trimethylphenylamino)-6-(3,5-dimethylphenoxy)-1,3,5-triazine (11) 2-Methylamino-4-mexylamino-6-(3,5-dimethylphenoxy)-1,3,5-triazine (1.00 g, 2.86 mmol) was dissolved in anhydrous DMF (10 mL) in a flame-dried round-bottomed flask equipped with a magnetic stirrer. NaH (60 wt%, 0.172 g, 4.29 mmol) was added, and the mixture was stirred 30 min at ambient temperature until hydrogen evolution had stopped. Iodomethane (0.267 mL, 0.609 g, 4.29 mmol) was slowly added, and the mixture was stirred at ambient temperature for 12 h. Ethyl ether and H_2O were then added, and both layers were separated. The organic layer was recovered, washed with H_2O and brine, dried over Na_2SO_4, filtered, and the volatiles were evaporated under vacuum. The product was purified by recrystallization from hot hexanes to give 0.651 g of compound **11** (1.79 mmol, 63 %). T_g 33 °C, T_c 126 °C, T_m 152 °C; FT-IR (ATR/CH_2Cl_2) 3421, 3267, 3179, 3140, 3011, 2946, 2918, 2866, 1606, 1576, 1539, 1492, 1427, 1405, 1386, 1358, 1322, 1291, 1266, 1232, 1218, 1191, 1167, 1146, 1132, 1116, 1055, 1033, 999, 977, 950, 931, 907, 888, 846, 810, 736, 695, 685 cm^{-1}; ^{1}H NMR (400 MHz, DMSO-d_6, 363 K) δ 6.97 (br s, 1H), 6.91 (s, 2H), 6.84 (s, 1H), 6.80 (s, 1H), 6.75 (s, 2H), 3.38 (s, 3H), 2.76 (d, ^3J = 4.3 Hz, 3H), 2.26 (s, 12H) ppm; ^{13}C NMR (75 MHz, DMSO-d_6) δ 170.6, 167.8, 167.3, 166.9, 166.5, 152.7, 152.7, 144.5, 144.4, 138.9, 138.5, 138.1, 137.9, 127.5, 126.6, 124.6, 119.6, 38.0, 27.5, 21.2 ppm; HRMS (ESI, MNa$^+$) calcd. for $C_{21}H_{26}N_5O$ m/e: 364.2132, found: 364.2142.

2-Methoxy-4-(N,3,5-trimethylphenylamino)-6-(3,5-dimethylphenoxy)-1,3,5-triazine (12) 2-Methoxy-4-mexylamino-6-(3,5-dimethylphenoxy)-1,3,5-triazine (1.00 g, 2.85 mmol) was dissolved in anhydrous DMF (10 mL) in a flame-dried round-bottomed flask equipped with a magnetic stirrer. NaH (60 wt%, 0.171 g, 4.28 mmol) was added, and the mixture was stirred 30 min at ambient temperature until hydrogen evolution had stopped. Iodomethane (0.266 mL, 0.608 g, 4.28 mmol) was slowly added, and the mixture was stirred at ambient temperature for 12 h. Ethyl ether and H_2O were then added, and both layers were separated. The organic layer was recovered, washed with H_2O and brine, dried over Na_2SO_4, filtered, and the volatiles were evaporated under vacuum. The product was purified by recrystallization from hot hexanes to give 0.640 g of compound **12** (1.76 mmol, 62 %). T_g 8 °C, T_m 129 °C; FT-IR (ATR/CH_2Cl_2) 3012, 2952, 2919, 2867, 1607, 1574, 1534, 1468, 1412, 1363, 1321, 1292, 1260, 1228, 1199, 1184, 1146, 1121, 1101, 1055, 1000, 931, 888, 848, 813, 713, 697, 684 cm^{-1}; ^{1}H NMR (400 MHz, DMSO-d_6, 363 K) δ 6.92 (s, 2H), 6.89 (s, 1H), 6.84 (s, 1H), 6.77 (s, 2H), 3.81 (s, 3H), 3.40 (s, 3H), 2.27 (s, 12H) ppm; ^{13}C NMR (75 MHz, DMSO-d_6) δ 172.2, 171.8, 167.5, 152.2, 143.6, 138.9, 138.3, 128.2, 128.1, 127.2, 127.0, 124.4, 124.3, 119.5, 119.4, 54.7,

38.4, 38.3, 21.2 ppm; HRMS (ESI, MNa$^+$) calcd. for $C_{21}H_{24}NaN_4O_2$ *m/e*: 387.1791.1642, found: 387.1802.

Acknowledgements

Notes and references

‡ Marvin was used for drawing, displaying and characterizing chemical structures, substructures and reactions (Schemes 1; 3-5 and S1), Marvin 6.0.0, 2013, ChemAxon (http://www.chemaxon.com).
§ mexyl = 3,5-diphenyl

1   Ediger, M. D., Angell, C. A., Nagel, S. R. *J. Phys. Chem.* **1996,** *100*, 13200.
2   Kulkarni, A. P., Tonzola, C. J., Babel, A., Jenekhe, S. A. *Chem. Mater.* **2004,** *16*, 4556.
3   Hancock, B. C., Zografi, G. *J. Pharm. Sci.* **1997,** *86*, 1.
4   Alba, C., Busse, L. E., List, D. J., Angell, C. A. *J. Chem. Phys.* **1990,** *92*, 617.
5   Whitaker, C. M., McMahon, R. J. *J. Phys. Chem.* **1996,** *100*, 1081.
6   Ping, W., Paraska, D., Baker, R., Harrowell, P., Angell, C. A. *J. Phys. Chem. B* **2011,** *115*, 4696.
7   Liu, T., Cheng, K., Salami-Ranjbaran, E., Gao, F., Glor, E. C., Li, M., Walsh, P. J., Fakhraai, Z. *Soft Matter* **2015**.
8   Lebel, O., Maris, T., Perron, M.-È., Demers, E., Wuest, J. D. *J. Am. Chem. Soc.* **2006,** *128*, 10372.
9   Desiraju, G. R. *Acc. Chem. Res.* **2002,** *35*, 565.
10 Wuest, J. D. *Chem. Commun.* **2005**, 5830.
11 Wicker, J. G. P., Cooper, R. I. *CrystEngComm* **2015,** *17*, 1927.
12 Carvalho, S. P., Wang, R., Wang, H., Ball, B., Lebel, O. *Cryst. Growth Des.* **2010,** *10*, 2734.
13 Eren, R. N., Plante, A., Meunier, A., Laventure, A., Huang, Y., Briard, J. G., Creber, K. J., Pellerin, C., Soldera, A., Lebel, O. *Tetrahedron* **2012,** *68*, 10130.
14 Laventure, A., Soldera, A., Pellerin, C., Lebel, O. *New J. Chem.* **2013,** *37*, 3881.
15 Plante, A., Mauran, D., Carvalho, S. P., Pagé, J. Y. S. D., Pellerin, C., Lebel, O. *J. Phys. Chem. B* **2009,** *113*, 14884.
16 Plante, A., Palato, S., Lebel, O., Soldera, A. *J. Mater. Chem. C* **2013,** *1*, 1037.
17 Naito, K. *Chem. Mater.* **1994,** *6*, 2343.
18 van der Sman, R. G. *J. Phys. Chem. B* **2013,** *117*, 16303.
19 Zhang, L., Xu, S., Yang, Z., Cao, S. *Mater. Chem. Phys.* **2011,** *126*, 804.
20 Kamino, B. A., Castrucci, J., Bender, T. P. *Silicon* **2011,** *3*, 125.
21 Risen Jr, W. M. *J. Non-Cryst. Solids* **1985,** *76*, 97.
22 Tang, X., Pikal, M., Taylor, L. *Pharm. Res.* **2002,** *19*, 477.

23 Imamura, K., Sakaura, K., Ohyama, K.-i., Fukushima, A., Imanaka, H., Sakiyama, T., Nakanishi, K. *J. Phys. Chem. B* **2006,** *110*, 15094.
24 Baran, J., Davydova, N. A., Pietraszko, A. *J. Mol. Struct.* **2005,** *744–747*, 301.
25 Costard, R., Greve, C., Fidder, H., Nibbering, E. T. *J. Phys. Chem. B* **2015,** *119*, 2711.
26 Gemperline, P. *Practical Guide To Chemometrics*. 2nd ed.; CRC Press: Boca Raton, 2006.
27 Windig, W., Guilment, J. *Anal. Chem.* **1991,** *63*, 1425.
28 Windig, W., Stephenson, D. A. *Anal. Chem.* **1992,** *64*, 2735.
29 Libnau, F. O., Toft, J., Christy, A. A., Kvalheim, O. M. *J. Am. Chem. Soc.* **1994,** *116*, 8311.
30 Segtnan, V. H., Šašić, Š., Isaksson, T., Ozaki, Y. *Anal. Chem.* **2001,** *73*, 3153.
31 Šašić, S., Segtnan, V. H., Ozaki, Y. *J. Phys. Chem. A* **2002,** *106*, 760.
32 Angell, C. A., Rodgers, V. *J. Chem. Phys.* **1984,** *80*, 6245.
33 Wang, R., Pellerin, C., Lebel, O. *J. Mater. Chem.* **2009,** *19*, 2747.
34 Garcia, D., Starkweather, H., Jr. Hydrogen Bonding in Nylon 66 and Model Compounds. In *Fourier Transform Infrared Characterization of Polymers*, Ishida, H., Ed. Springer US: 1987; Vol. 36, pp 213.
35 Barlow, S. J., Bondarenko, G. V., Gorbaty, Y. E., Yamaguchi, T., Poliakoff, M. *J. Phys. Chem. A* **2002,** *106*, 10452.
36 Harvey, J. A., Auerbach, S. M. *J. Phys. Chem. B* **2014**.
37 Harvey, J. A., Basak, D., Venkataraman, D., Auerbach, S. M. *Mol. Phys.* **2012,** *110*, 957.
38 Kaminski, K., Kipnusu, W. K., Adrjanowicz, K., Mapesa, E. U., Iacob, C., Jasiurkowska, M., Wlodarczyk, P., Grzybowska, K., Paluch, M., Kremer, F. *Macromolecules* **2013,** *46*, 1973.
39 Angell, C. A., Alba-Simionesco, C., Fan, J., Green, J. L. Hydrogen Bonding and the Fragility of Supercooled Liquids and Biopolymers. In *Hydrogen Bond Networks*, Bellissent-Funel, M.-C.; Dore, J., Eds. Springer Netherlands: 1994; Vol. 435, pp 3.
40 Steiner, T. *Angew. Chem. Int. Ed.* **2002,** *41*, 48.
41 Pawlus, S., Grzybowski, A., Paluch, M., Wlodarczyk, P. *Phys. Rev. E* **2012,** *85*, 052501.
42 Vaupel, S., Brutschy, B., Tarakeshwar, P., Kim, K. S. *J. Am. Chem. Soc.* **2006,** *128*, 5416.
43 Bloom, J. W. G., Raju, R. K., Wheeler, S. E. *J. Chem. Theory Comput.* **2012,** *8*, 3167.
44 Wheeler, S. E., Bloom, J. W. *J. Phys. Chem. A* **2014,** *118*, 6133.
45 Mahlin, D., Ponnambalam, S., Heidarian Höckerfelt, M., Bergström, C. A. S. *Mol. Pharm.* **2011,** *8*, 498.
46 Yu, L., Reutzel-Edens, S. M., Mitchell, C. A. *Org. Process Res. Dev.* **2000,** *4*, 396.
47 Karis, T. E., Kim, S. J., Gendler, P. L., Cheng, Y. Y. *J. Non-Cryst. Solids* **1995,** *191*, 293.
48 Cenedese, S., Zhurov, V. V., Pinkerton, A. A. *Cryst. Growth Des.* **2015,** *15*, 875.
49 Tanaka, T., Noguchi, M., Watanabe, K., Misawa, T., Ishihara, M., Kobayashi, A., Shoda, S.-i. *Org. Biomol. Chem.* **2010,** *8*, 5126.
50 Dudley, J. R., Thurston, J. T., Schaefer, F. C., Holm-Hansen, D., Hull, C. J., Adams, P. *J. Am. Chem. Soc.* **1951,** *73*, 2986.
51 Kober, E., Rätz, R. *J. Org. Chem.* **1962,** *27*, 2509.
52 Matsuno, T., Kato, M., Tsuchida, Y., Takahashi, M., Yaguchi, S., Terada, S. *Chem. Pharm. Bull.* **1997,** *45*, 291.
53 Fusco, R., Sannicolo, F. *J. Org. Chem.* **1982,** *47*, 1691.
54 Frisch, M. J.; Trucks, G. W.; Schlegel, H. B.; Scuseria, G. E.; Robb, M. A.; Cheeseman, J. R.; Zakrzewski, V. G.; Montgomery, J. J. A.; Stratmann, R. E.; Burant, J. C.; Dapprich, S.; Millam, J. M.;

Daniels, A. D.; Kudin, K. N.; Strain, M. C.; Farkas, O.; Tomasi, J.; Barone, V.; Cossi, M.; Cammi, R.; Mennucci, B.; Pomelli, C.; Adamo, C.; Clifford, S.; Ochterski, J.; Petersson, G. A.; Ayala, P. Y.; Cui, Q.; Morokuma, K.; Malick, D. K.; Rabuck, A. D.; Raghavachari, K.; Foresman, J. B.; Cioslowski, J.; Ortiz, J. V.; Stefanov, B. B.; Liu, G.; Liashenko, A.; Piskorz, P.; Komaromi, I.; Gomperts, R.; Martin, R. L.; Fox, D. J.; Keith, T.; Al-Laham, M. A.; Peng, C. Y.; Nanayakkara, A.; Challacombe, M. W.; Gill, P. M.; Johnson, B.; Chen, W.; Wong, M. W.; Andres, J. L., Gonzalez, C.; Head-Gordon, M.; Replogle, E. S.; Pople, J. A. *Gaussian 98*, Revision A.6, Gaussian, Inc., Pittsburgh PA, **1998**.